

THE EFFECT OF PRIMORDIAL BLACK HOLES AND STREAMING MOTIONS ON STRUCTURE FORMATION.

F. ATRIO-BARANDELA¹*Draft version October 4, 2022*

ABSTRACT

Primordial Black Holes could be an important component of the dark matter in the Universe. If they exist, they would add a Poisson component to the matter power spectrum. The extra power would speed up the emergence of dark matter halos that seed the formation of first stars and galaxies. Kashlinsky (2021) suggested that the additional velocity fluctuations would accelerate the infall of baryons onto the dark matter potential wells. We analyze the effect of Primordial Black Holes on the baryon infall from recombination to reionization and find the correction to be a few percent of the power suppression first identified by Tseliakhovich & Hirata (2010). However, the dynamical effect of this correction in addition to the extra power speeds up the formation of halos in the mass range of $10^4 - 10^{5-6} M_{\odot}$, while slightly decreasing the formation of those in the range $10^6 - 10^8 M_{\odot}$ confirming earlier analytic estimates and recent results of numerical simulations.

Subject headings: (cosmology:) dark ages, reionization, first stars, (cosmology:) dark matter, (cosmology:) large-scale structure of universe

1. INTRODUCTION.

The detection of gravitational waves (GWs) by the LIGO and VIRGO observatories (Abbott et al. 2016, Abbott et al. 2020) originating from the merger of binary black hole (BH) systems revived the idea that Primordial Black Holes (PBHs) could constitute a large fraction, if not all, of the dark matter (DM) in the Universe (Bird et al. 2016, Clesse & García-Bellido 2016, Kashlinsky 2016, Carr, Clesse & García-Bellido 2021). Such PBHs could have originated during the QCD epoch (Jedamzik 1997). The detected binary BH mergers were unlikely to be composed of BHs with large spins aligned to the orbital angular momentum as one could expect from stellar BHs (Abbott et al. 2019). Particularly interesting were those PBHs in the mass range $M_{PBH} \sim 10 - 50 M_{\odot}$ as they could be the source of the binary BH events detected by LIGO/VIRGO. The event rate can be fitted by a combined population of PBHs and stellar BH mergers (Franciolini et al. 2022) but models where all the DM is composed of PBHs also match the LIGO/Virgo observed merger rates (Jedamzik 2021). In parallel, astrophysical constraints have limited the mass range and fraction of PBHs (Lacki & Beacom 2010, Ali-Haïmoud & Kamionkowski 2017, Poulin et al. 2017, Oguri et al. 2018, Laha 2019, Blaineau, Moniez & Afonso 2022) and current estimates in the mass range of interest limit the fraction of PBHs to be $f_{PBH} \sim 10^{-4} - 0.1$ (Carr & Kühnel 2020) although those constraints could be weakened if PBHs are clustered (Belotsky et al 2019) and/or have an extended mass function. Carr et al. (2021) argued that a multi-modal PBH mass spectrum would make compatible $f_{PBH} \sim 1$ with astronomical constraints. Kashlinsky, Ali-Haïmoud, Clesse et al. (2019) discussed the prospects that new instruments and observations in the coming years could probe the existence of PBHs and determine their fraction in the DM component.

A population PBHs would add a Poisson isocurvature component to the adiabatic matter density perturbations generated during inflation. This contribution would dominate the power at small scales (Meszaros 1975, Afshordi, McDonald & Spergel 2003), increasing the abundance of early dark matter halos. At each redshift, the increment on the number density of collapsing halos would result in a more efficient formation of first stars and galaxies, helping to explain the level of source-subtracted cosmic infrared background (CIB) fluctuations (Kashlinsky 2016) that cannot be accounted for by the known galaxy populations (Kashlinsky et al. 2005, 2007). Furthermore, baryon accretion onto the population of PBHs would contribute to various cosmic backgrounds and explain, for instance, the coherence of the X-ray and near-infrared backgrounds (Cappelluti et al. 2013, Cappelluti et al. 2017, see Kashlinsky et al. 2018 for a review). Detailed studies of the emission over cosmic time from star formation and black hole accretion in a PBH-DM universe have shown the viability of this type of models (Hasinger, 2020; Cappelluti, Hasinger & Natarajan 2021).

In this work we will consider the effect of a PBHs on the evolution of matter density perturbations and the formation of DM halos during reionization. After matter radiation equality, DM density perturbations grow while baryons and photons are still tightly coupled; later, at recombination, baryons fall into the DM potential wells. The baryonic sound speeds falls to $\sim 6 \text{ km s}^{-1}$ while the DM moves at $\sim 30 \text{ km s}^{-1}$. Tseliakhovich & Hirata (2010, hereafter TH) noticed that the supersonic motion of baryons relative to the DM rest frame suppressed the abundance of halos.

¹ Física Teórica. Universidad de Salamanca. 37008 Salamanca, Spain; atrio@usal.es

Baryons do not fall into the DM potential wells as fast as they would without the velocity effect resulting in linear fluctuations in the matter density being suppressed. The scales most affected were $k \sim 200h/\text{Mpc}$ and the effect was soon confirmed by numerical simulations (O’Leary & McQuinn, 2012). The effect of streaming velocities (advection) on the formation of DM halos and stellar objects has been extensively considered (Maio, Koopmans & Ciardi 2011, Tseliakhovich, Barkana & Hirata 2011, Richardson, Scannapieco & Thacker 2013) concluding that the formation of halos in the mass range $(10^4, 10^8)M_\odot$ were suppressed. Stacy, Bromm & Loeb (2011) also identified that when a halo is formed it does not contain a gas core as dense as it would have without advection. Nevertheless, the subsequent collapse of the gas and the formation of Pop III stars was very similar to the no-streaming case. Kashlinsky (2021) was the first to point out that PBHs would lead to a more efficient redistribution of kinetic energy between baryons and DM on the scales relevant for the formation of the first sources but did not quantify the amplitude of this effect. The details of the baryonic infall process are of great importance for understanding star formation and the evolution of the interstellar medium at redshifts $z > 10$. The reionization epoch could be directly probed through the absorption of the 21cm line (see Barkana 2016 for a review) and indirectly through the residual CIB fluctuations in source subtracted maps in the near infrared (NIR) (Kashlinsky et al. 2018). Both probes could, consequently, test the effect of streaming velocities and PBHs. If the latter play an important role on the collapse of early halos then the physical effects during reionization generated by this population could be observable with forthcoming data (Kashlinsky, Arendt, Cappelluti et al. 2019, Hasinger 2020, Cappelluti et al. 2021).

Numerical simulations have only recently started to consider the effect of streaming motions and PBHs on the formation of first stars. Liu, Zhang & Bromm (2022) compared the results of two simulations with streaming motions, with and without PBHs and found that the effect of streaming motions were weaker with PBHs. In this article we analyze how PBHs alter the evolution of matter density perturbations in the presence of streaming motions. We will consider $f_{PBH} \sim 10^{-3} - 1$ and an effective mass of $M_{PBH} = 30M_\odot$. In Sec. 2 we summarize the TH formalism. In Sec. 3 we present our main results and discuss their implications and in Sec. 4 we summarize our main conclusions.

2. FORMALISM.

On scales of a few Mpc, the DM (assumed to be cold dark matter, CDM) moves with a bulk velocity of $\sim 30\text{km/s}$ when the baryon sound speed is $\sim 6\text{km/s}$. The velocity difference is generated by large scale modes of wavelength up to $\sim 200\text{Mpc}$. On scales smaller than $\sim 1\text{Mpc}$ baryons are subject to a uniform and supersonic motion (Mach number $\mathcal{M} \sim 5$) in the DM rest frame. These regions are the background where smaller scale density perturbations grow due to gravitational instability. TH showed that in this scenario the equations describing the evolution of matter perturbations at first order contain non-linear terms that change the conclusions of linear theory.

Newtonian theory accurately describes the evolution of subhorizon density perturbations of baryons and DM in the matter dominated regime, when fluctuations in the radiation field can be ignored (Peebles 1980). In the presence of uniform streaming motions, the background motion of baryons and DM can be separated from the peculiar velocity of small scale perturbations by writing $\vec{v}_j(\vec{x}, t) = \vec{v}_j^{(bg)}(t) + \vec{u}_j(\vec{x}, t)$, where the super index (*bg*) denotes the background (streaming) motion between baryons and DM within the patch. If PBHs were present in the early Universe, they will affect the velocity field by adding an isocurvature component to the DM power spectrum. In order to apply the TH formalism we need to demonstrate that baryons and PBHs are still moving coherently with respect to each other on patches of a few Mpc.

Let $\delta_j = (\rho_j - \bar{\rho}_j)/\bar{\rho}_j$ denote the density contrast of a matter component and \vec{v}_j its peculiar velocity; $j = (b, c)$ where (*b*) refers to baryons and (*c*) to DM. Peculiar velocities are related to matter density perturbations as

$$\vec{v}_j(\vec{k}) = -i \frac{H}{(1+z)} \frac{d \ln D}{d \ln z} \delta_j(\vec{k}, t) \frac{\vec{k}}{k^2}, \quad (1)$$

where density perturbations are written as $\delta_j(\vec{k}, z) = D_j(z) \delta_j(\vec{k})$. The growth factor $D_j(z)$ gives the time evolution of density perturbation of baryons and DM; $H = H_0 E(z)$ and $E^2(z) = \Omega_m(1+z)^3 + \Omega_r(1+z)^4 + \Omega_\Lambda$. $H_0, \Omega_m, \Omega_r, \Omega_\Lambda$ are the current values of the Hubble constant, the matter and radiation energy densities and the energy density associated with the cosmological constant Λ . Let us denote the logarithmic growth by $F_j = d \ln D_j / d \ln z$. The variance of the streaming velocity field between baryons and dark matter can be written as

$$v_{bc}^2 = \langle \vec{v}_{bc} \cdot \vec{v}_{bc} \rangle = \int_0^\infty \frac{k^3 |\vec{v}_{bc}|^2 dk}{2\pi^2 k} = \int_0^\infty \Delta_{v,bc}^2(k) d \ln k. \quad (2)$$

The square fluctuation streaming velocity power per logarithmic k-interval is

$$\Delta_{v,bc}^2(k) = \frac{1}{2\pi^2} \frac{H^2}{(1+z)^2} k (F_b \delta_b - F_c \delta_c)^2. \quad (3)$$

It gives the contribution to the variance of the streaming velocity field per unit interval in $\ln k$. F_b, F_c are the logarithmic growth functions for baryons and DM, respectively.

PBHs add an extra contribution to the matter power spectrum due to the fluctuation on the number density of PBHs. The power spectrum is constant, independent of scale and is given by (Afshordi et al. 2003)

$$P_{PBH}(k) = \frac{9}{4} \left(\frac{1 + z_{eq}}{D_+(z)} \right)^2 \frac{M_{PBH}}{f_{PBH} \rho_{cr} \Omega_c} \approx 1.26 \times 10^{-8} \left(\frac{1330}{D_+(1020)} \right)^2 \left(\frac{M_{PBH}}{30 M_\odot} \right) \left(\frac{1}{f_{PBH}} \right) \left(\frac{0.125}{\Omega_c h^2} \right) \text{Mpc}^{-3} \quad (4)$$

where $z_{eq} \approx 3413$ is the redshift of matter radiation equality, $D_+(z)$ is the linear growth factor of matter density perturbations from redshift z till today normalized to unity at present, M_{PBH} is the effective mass of PBHs, f_{PBH} is the fraction of DM that is composed of PBHs, ρ_{cr} is the critical density and Ω_c is the fraction of the energy density that is made of DM particles (including PBHs).

Fig. 1 plots the contribution of the different scales to the variance of the velocity difference between baryons and DM. The solid (black) line represents the streaming velocity variance, given by eq. (3), of the concordance Λ CDM model with densities $\Omega_c = 0.255$, $\Omega_b = 0.0455$, Hubble parameter $h = 0.7$ and spectral index at large scales $n_s = 0.98$. The dashed (blue), the dot-dashed (red), the triple dot-dashed (green) and the long dashed (gold) lines corresponds to PBHs fractions $f_{PBH} = 1, 0.1, 0.01, 10^{-3}$, respectively. Plots correspond to redshift $z = 1020$. In the matter dominated regime the logarithmic growth factors are $F_c \approx F_b \approx 1$. However, the contribution of the radiation energy density to the background expansion is not negligible near decoupling. For a more accurate treatment, we obtained the logarithmic growth factors using the baryon and CDM transfer functions at redshifts $z_1 = 1020$ and $z_2 = 1010$, computed using the CMBFAST code (Seljak & Zaldarriaga, 1996). Fig. 1 demonstrates that the streaming velocity is still dominated by contributions coming from scales in the range $k \in [0.01, 1] h\text{Mpc}^{-1}$. The effect of PBHs depends on f_{PBH} and it is only relevant at $k \geq 50 h\text{Mpc}^{-1}$. Beyond this scale, the constant matter power spectrum from PBHs results on the streaming velocity variance growing as $\Delta_{v,bc}^2(k) \propto k$. It could be expected that for scales $k \geq 1 h\text{kpc}^{-1}$ the random motion induced by PBHs would disrupt the uniform supersonic motion of baryons in the DM rest frame. Numerical simulations have shown that the presence of PBHs gives rise to a significant nonlinear effect that it is not present in the standard Λ CDM model, damping the matter power spectrum compared with the expectation from linear theory (see Fig 4 of Inman & Ali-Haïmoud 2019). By $z = 100$, the matter power spectrum is damped on scales $k \geq 0.2 h\text{kpc}^{-1}$ when the fraction of PBHs is larger than $f_{PBH} \geq 0.1$. Therefore, the homogeneity of the streaming baryon flow in the DM rest frame will not be disrupted. For $f_{PBH} < 0.1$, the evolution is well described by linear theory but the contribution of PBHs at $k \geq 1 h\text{kpc}^{-1}$ is much smaller than the contribution from $k \geq 1 h\text{Mpc}^{-1}$. In summary, the random motions induced by the PBHs power spectrum will not cancel the effect of DM-baryon supersonic motion and the decomposition of the velocity field into a uniform background motion and a peculiar velocity field at small scales can be applied for any fraction of PBHs.

The equations of evolution baryons and DM density perturbations of a mode with wavenumber \vec{k} and in the matter dominated regime are given by (TH, eqs. 11)

$$\begin{aligned} \frac{\partial \delta_c}{\partial t} &= \frac{i}{a} \vec{v}_{bc}^{(bg)} \cdot \vec{k} \delta_c - \theta_c \\ \frac{\partial \theta_c}{\partial t} &= \frac{i}{a} \vec{v}_{bc}^{(bg)} \cdot \vec{k} \theta_c - \frac{3}{2} H^2 (\Omega_c \delta_c + \Omega_b \delta_b) - 2H \theta_c \\ \frac{\partial \delta_b}{\partial t} &= -\theta_b \\ \frac{\partial \theta_b}{\partial t} &= -\frac{3}{2} H^2 (\Omega_c \delta_c + \Omega_b \delta_b) - 2H \theta_c + \frac{c_s^2 k^2}{a^2} \delta_b \end{aligned} \quad (5)$$

where θ is the divergence of the peculiar velocity field \vec{u}_j , given by $\vec{u}_j = -ia(\vec{k}/k^2)\theta(\vec{k})$. These equations are written in the baryon rest frame but they could have been equally written in the DM rest frame (O'Leary & McQuinn 2012). TH solved these equations assuming perturbations evolved in a background where baryon and DM densities were equal to the mean. On these regions the background velocities would be constant in position but their amplitudes would decrease in time with the scale factor $a(t)$ as $\vec{v}_b^{(bg)}, \vec{v}_c^{(bg)} \sim a^{-1}$. Their relative velocity would scale similarly, $\vec{v}_{bc}^{(bg)} = (\vec{v}_b^{(bg)} - \vec{v}_c^{(bg)}) \sim a^{-1}$. Ahn (2016) showed that the relative velocity $\vec{v}_{bc}^{(bg)}$ scaled as the inverse of the scale factor even if the baryon and DM densities of the background were not the mean density, so we will use eqs. (5) from TH instead of a more general treatment. The effect of the bulk motion in eqs. (5) is encoded in the terms containing the streaming velocity factor $\vec{v}_{bc}^{(bg)}$, since if $\vec{v}_{bc}^{(bg)} = 0$ eqs. (5) would simply describe the evolution of matter density perturbation in the linear regime.

3. NUMERICAL RESULTS AND DISCUSSION.

We solved numerically eqs. (5) to determine the contribution of PBHs to the advection of small scale perturbations by the DM streaming motions. At redshift $z = 1020$ the r.m.s streaming velocity is $v_{bc}^{(bg)} \approx 30 \text{ km/s}$; adding the PBHs component increases this amplitude by a 0.1%. For a better understanding of the effect of PBHs, we fixed $v_{bc}^{(bg)} = 30 \text{ km/s}$ in both the standard model and in models including PBHs. The numerical solution will depend on

the cosine of the angle between the direction of the bulk flow velocity $\vec{v}_{bc}^{(bg)}$ and the wavenumber \vec{k} . We follow TH and define the isotropic average fluctuation power per logarithmic interval, or variance, as

$$\Delta_m^2(k) = \frac{1}{2} \int_{-1}^1 \Delta_m^2(k, \cos \theta) d \cos \theta \quad (6)$$

where $\Delta_m^2(k) = k^3 P(k)/2\pi^2$ and $P(k) = |\delta_m(k)|^2$ is the matter power spectrum that includes the baryon, DM and PBHs components, i.e., $\delta_m = \delta_c + \delta_b + \delta_{PBH}$. $\Delta_m^2(k, \cos \theta)$ is the same magnitude for each angle θ between the background bulk flow velocity $\vec{v}_{bc}^{(bg)}$ and \vec{k} . We computed the effect at redshifts $z = 20, 40, 60$ and 80 and the results are presented in Fig. 2. In the matter regime Δ_m scales linearly with redshift in the absence of advection. In Fig. 2a we plot $\Delta_m^2(k) * (1+z)^2$ to show the effect of advection at different redshifts. To avoid clutter, we plot only $z = 20, 80$ that bracket the variation with redshift. Lines correspond to $f_{PBH} = 1, 0.1, 10^{-2}, 10^{-3}, 0$ from left to right and are shown with blue, green, red, gold and black lines, respectively. Solid lines correspond to no-advection and broken lines to advection. The triple dot-dashed line corresponds to $z = 20$ and the dashed line to $z = 80$. The figure shows that at any redshift PBHs increase the power at small scales and their effect on advection is second order; in most cases the differences can not be seen. In Fig. 2b we plot the relative differences between the variances. Solid lines correspond to $f_{PBH} = 0$ and the triple dot-dashed lines to $f_{PBH} = 1$. Again, to avoid clutter we do not plot the result for other fractions since they will fall between the two cases represented in the plot. From top to bottom, lines correspond to $z = 20$ (black), $z = 40$ (blue), $z = 60$ (red) and $z = 80$ (green). When all other parameters are kept fixed, the relative effect of PBHs is a few percent that, combined with the added power, gives rise to significant differences in the number density of objects as we shall discuss in the next section. In Fig. 2c we represent the variance ratio of advection to no-advection. From top to bottom, pairs of lines correspond to $z = 80, 60, 40$ and 20 , coded by color as green, red, blue and black, respectively. Solid lines correspond to no-advection and triple dot-dashed lines to advection with $f_{PBH} = 1$. All other fractions fall between the two plotted cases. Unity indicates that advection does not affect the evolution of density perturbations.

The advection velocity is, on average, $v_{bc}^{(bg)} = 30\text{km/s}$, but it will vary from one patch to the next. In Fig. 2d we show the effect on the variance ratio when changing the amplitude of the baryon-dark matter streaming velocity. Solid (blue) lines correspond to $z = 80$ and triple dot-dashed lines to $z = 20$. In each group, top, middle and bottom lines correspond to velocities $v_{bc}^{(bg)} = 20, 30$ and 40km/s , respectively. As expected, the larger the velocity, the stronger the effect of advection.

More significant than the correction for advection is the extra power at small scales added by PBHs. This extra power increases the rate of formation of matter halos at early times (Kashlinsky 2016). To estimate the effect of PBHs on the formation of halos in the presence of streaming motions, we will use the Press-Schechter formalism (Press & Schechter, 1974). The number density of objects dn that are collapsing at redshift z per unit of mass is a function of the r.m.s. mass fluctuation $\sigma(M)$ and is given by

$$\frac{dn}{dM} = \sqrt{\frac{2}{\pi}} \frac{\bar{\rho}_m}{M^2} \frac{\delta_c}{\sigma_M} \left| \frac{d \ln \sigma_M}{d \ln M} \right| \exp \left(-\frac{\delta_c^2}{2\sigma_M^2} \right) \quad (7)$$

where $\bar{\rho}_m$ is the mean matter density, $\delta_c = 1.686$ the critical overdensity above which a given mass fluctuation collapse and

$$\sigma_M^2(R) = \int_0^\infty \Delta_m^2(k) W^2(kR) d \ln k \quad (8)$$

where $\Delta_m^2(k)$ is given in eq. (6). The variance of the matter density field σ_M is computed on spheres of radius $R = (3M/4\pi\bar{\rho}_m)$ and $W(x) = 3j_1(x)/x$ is the Fourier transform of the top hat window function.

We compute the number density of objects in the range $[10^4, 10^8]h^{-1}M_\odot$, where advection suppresses the formation of matter halos the most. Eq. (7) assumes that density perturbations are gaussian. However PBHs are Poisson distributed and the density field will not be gaussian, mainly at the scales where the PBH contribution dominates. The power average in eq. (6) will have the same statistical distribution than $\Delta_m^2(k, \cos \theta)$. The average will not dilute the non-gaussianity due to PBHs and, consequently our treatment can only be considered an approximation. Numerical simulations are needed to provide a more accurate estimate of the effect of PBHs on the number density of matter halos. Our results are presented in Fig. 3. We plot the ratio of the number densities (given by eq. 7) of models with advection to models without advection as a function of halo mass. The mass scale is related to wavenumber as $k = 2\pi(4\pi\bar{\rho}_m/3M)^{1/3} \approx 95(10^8 h^{-1}M_\odot/M)^{1/3} h\text{Mpc}^{-1}$. The formation of halos at $M \sim 10^4 h^{-1}M_\odot$ are dominated by scales $k \sim 2h\text{kpc}^{-1}$. As indicated, at those scales the non-linear evolution of PBHs damps the matter power spectrum (Inman & Ali-Haïmoud 2019). This non-linear effect can only be estimated from simulations and we simplify the non-linear evolution by extrapolating the matter power spectrum linearly from its amplitude at $k = 1h\text{kpc}^{-1}$ in the region $k \geq 1 - 10h\text{kpc}^{-1}$. Figs. 3a-d correspond to redshifts $z = 80, 60, 40$ and 20 , respectively. Dashed (blue), dot-dashed (red), triple dot-dashed (green), long-dashed (gold) and solid (black) lines correspond to PBHs fractions $f_{PBH} = (1, 0.1, 0.01, 10^{-3}, 0)$. Comparing the results at these four redshifts, we see that the effect of advection is diluted over time. This is expected since baryons and DM tend to move together with decreasing redshift.

The small correction that PBHs induced in the streaming motion of baryons is shown in Fig. 2, combined with the larger values of σ_8 due to the extra power on small scales result on a large increment on the number of low mass halos, as shown in Fig. 3. At these small scales $\sigma(M) \sim 2 - 10$ and the exponential factor in eq. (7) is close to unity. The abundance of objects is dominated by σ_M^{-2} at a fixed mass. Since the variance of the density field with advection is smaller than without advection, the number density of objects is larger, resulting in a significant enhancement on the abundance of the less massive halos with respect to the standard model of DM particles. Fig. 3 shows that in the considered redshift range, PBHs help the formation of halos with masses $M \leq 10^{5-6} h^{-1} M_\odot$ in the presence of baryon advection. In the high mass end, the situation is reversed, with PBHs suppressing the formation of halos. Fig. 3 also shows that when $f_{PBH} \sim 1$, objects in the range $M \sim 10^4 M_\odot$ are formed more efficiently with than without advection. This result can not be trusted due to our oversimplified treatment. First, as we have already indicated, numerical simulations showed that non-linear evolution suppresses the isocurvature component of the DM power spectrum (Inman & Ali-Haïmoud 2019), effect that we did not take into account. Second, at these scales the PBHs dominate the matter power spectrum and the Press-Schechter estimates are less accurate since density fluctuations depart from gaussianity.

Halos, made of PBHs, would be subject to stellar dynamical evolution effects leading to super-massive BHs early on (Kashlinsky & Rees, 1983). Once formed, they would require efficient cooling mechanisms for baryons to collapse and form stars. Atomic cooling is efficient when the halo reaches a virial temperature of $T_{vir} = 10^4$, while molecular hydrogen, when present, provides efficient cooling down to temperatures $T_{vir} = 300\text{K}$ (Barkana & Loeb 2001). In Fig. 3 the vertical lines indicate the masses of matter halos with virial temperatures $T_{vir} = 10^3\text{K}$, left and 10^4K , right. In these estimates we have assumed that the gas in those halos was primordial. Since less massive halos are formed earlier and more abundantly, if all physical conditions are equal, the collapse of low mass halos and the formation of first stars within them will be favored by the presence of PBHs. Physically one expects that if density perturbations grow faster in the absence of streaming motions, it would also form objects more quickly. The interplay between the advection of baryons and the growth of density perturbations at low mass scales facilitates the formation of halos in the $10^4 - 10^5 h^{-1} M_\odot$ mass range. Since the Press-Schechter formalism gives only an approximate picture of the collapse of non-linear structures, numerical simulations are necessary to verify the correctness of this prediction. Liu et al. (2022) included one simulation with PBHs and streaming motions and found that the effect of advection was weaker with PBHs, concluding that the perturbations from PBHs accelerated the decoupling of baryons from the large scale flow. Their model had $f_{PBH} = 10^{-3}$ and the same BH masses and streaming velocities that in this work. Their simulation corresponds to the triple dot-dashed curves of Fig. 3 and their result agrees with our prediction that PBHs speed up the formation of objects in the range $(10^4 - 10^5) M_\odot$.

The suppression of small-scale baryonic structures due to streaming velocities will affect the post-reionization gas distribution, the gas temperature, the 21-cm line temperature, the large scale distribution of stars and will alter the 21-cm signal. Its power spectrum will show prominent Baryon Acoustic Oscillations (BAO) (Barkana 2016) reflecting the BAO signature in Fig. 1. The existence of PBHs will further blur this picture since they will enhance the formation of halos of mass $M \sim 10^4 - 10^5 M_\odot$ while decreasing slightly more the formation of more massive halos. The final effect will depend on the BH masses, mass distribution and their fraction.

4. CONCLUSIONS.

We have analyzed the effect of PBHs in the evolution of small scale baryon and DM density perturbations in the presence of streaming motions. TH found that the modes most strongly affected were those around $k \sim 200 h \text{Mpc}^{-1}$. PBHs add a constant isocurvature component to the matter density perturbations that dominates the power at small scales. This extra power induces a peculiar velocity field that does not disrupt the picture of the DM moving at decoupling at supersonic speed with respect to baryons. We have considered the power generated by PBHs of masses $M \sim 30 M_\odot$ and with fractions $f_{PBH} = 10^{-3} - 1$ in the total DM budget. We have found that PBHs favor the collapse of halos with mass $M \leq 10^5 - 10^6 M_\odot$ while slightly disfavor their formation for higher masses. We have quantified the amplitude of this effect, first predicted by Kashlinsky (2021). Since the less massive halos form earlier, the overall effect is to weaken the role of streaming motions in the evolution of matter density perturbation on Mpc scales, corroborating the result found by Liu et al. (2022) in their numerical simulations.

We have predicted that PBHs help halos of masses $10^4 - 10^5 M_\odot$ to collapse slightly more effectively in the presence of advection than in their absence. This shows the limitations of our model since in addition to non-linear effects and the non-gaussianity of the PBH power spectrum, we are not taking into account variations on the physical conditions of the gas, the cooling process or the feedback from PBH accretion. All those effects can only be verified with numerical simulations since the overall picture is unlikely to be as simple as described by our analytical model. If the ratio of PBHs to the total density of DM is small, one would expect PBHs to accrete large amounts of matter but contributing little to the matter power spectrum. When all the DM is made of BHs, the Poisson fluctuation in the PBHs number density would dominate the dynamics on small scales. Both regimes, termed "seed" and "Poisson" limits (Carr & Silk 2018) can be explored by analytical methods. For PBHs of masses $10 - 100 M_\odot$ and fractions $f_{PBH} = 10^{-3} - 0.1$ DM structures around individual PBHs will interact and their dynamics can only be followed with time consuming N-body simulations as in Inman & Ali-Haïmoud (2019). PBHs shift star formation to more massive halos, accelerating structure formation more strongly in regions with higher initial overdensities (Liu et al. 2022), physics that is not captured by our formalism. Still, analytical methods like the one presented here provide a general understanding of

the physical processes without expensive computations.

Acknowledgments: We thank A. Kashlinsky for discussions and we acknowledge financial support from grants PGC2018-096038-B-I00 (MINECO and FEDER, "A way of making Europe") and SA083P17 from the Junta de Castilla y León.

REFERENCES

- Abbott, B. P., Abbott, R., Abbott, T. D., et al. 2016, *Phys. Rev. Lett.*, 116, 061102
- Abbott B.P., Abbott, R., Abbott, T. D., et al. (LIGO Scientific, Virgo) 2019, *Phys. Rev. X*, 9, 031040
- Abbott, R., Abbott, T. D., Abraham, S., et al. (LIGO Scientific, Virgo) 2021, *Physical Review X*, 11, 021053
- Afshordi, N., McDonald, P. & Spergel, D. N. 2003, *ApJ*, 594, L71
- Ahn, K. 2016, *ApJ*, 830, 68
- Ali-Haïmoud, Y. & Kamionkowski, M. 2017, *Phys. Rev. D* 95, 043534
- Barkana, R. 2016, *Phys Rep*, 645, 1
- Barkana, R. & Loeb, A 2001, *Phys Rep*, 349, 125
- Belotskym K. M., Dokuchaev, V. I., Eroshenko, Yu. N., Esipova, E. A., Khlopov, M. Yu., Khromykh, L. A., Kirillov, A. A., Nikulin, V. V., Rubin, S. G. and Svadkovsky, I. V. (2019) *Eur. Phys. J. C*, 79, 246
- Bird, S., Cholis, I., Muñoz, J. B., et al. 2016, *Phys. Rev. Lett.*, 116, 201301
- Blaineau, T., Moniez, M. & Afonso, C. 2022, *Astron & Astrophys.*, 664, 106
- Cappelluti, N., Kashlinsky, A., Arendt, R. G., Comastri, A., Fazio, G. G., Finoguenov, A., Hasinger, G., Mather, J. C., Miyaji, T. & Moseley, S. H. 2013, *ApJ*, 769, 68
- Cappelluti, N., Arendt, R. G., Kashlinsky, A., Li, Y., Hasinger, G., Helgason, K., Urry, M., Natarajan, P. & Finoguenov, A. 2017, *ApJ*, 847, L11
- Cappelluti, N., Hasinger, H. & Natarajan, P. 2022, *Ap. J.*, 926, 205
- Carr, B., Clesse, S., García-Bellido, J. & Kühnel, F. 2021, *Phys. Dark Univ.*, 31, 100755
- Carr, B. & Kühnel, F. 2020, *Annual Review of Nuclear and Particle Science*, 70, 355
- Carr, B. & Silk, J. 2018, *MNRAS* 478, 3756
- Clesse, S. & García-Bellido, J. 2017, *Phys. Dark Univ.*, 15, 142
- Franciolini, G., Baibhav, V., De Luca, V. et al. 2022, *Phys. Rev. D*, 105, 083526
- Hasinger, G. 2020, *JCAP*, 07, 022
- Inman, D. & Ali-Haïmoud, Y. 2019, *Phys. Rev. D* 100, 083528
- Jedamzik, K. (1997) *Phys. Rev. D*, 55, 5871
- Jedamzik, K. (2021) *Phys. Rev. Lett.*, 126, 051302
- Kashlinsky, A. 2016, *ApJ*, 823, L25
- Kashlinsky, A. 2021, *Phys. Rev. Lett.*, 126, 011101
- Kashlinsky, A., Ali-Haimoud, Y., Clesse, S. et al. 2019, *Astro2020: Decadal Survey on Astronomy and Astrophysics. Bulletin of the American Astronomical Society*, 51, 51. arXiv:1903.04424
- Kashlinsky, A., Arendt, R. G., Atrio-Barandela, F., Cappelluti, N., Ferrara, A. & Hasinger, G. 2018, *Review of Modern Physics*, 90, 025006
- Kashlinsky, A., Arendt, R. G., Cappelluti, N., Finoguenov, A., Hasinger, G., Helgason, K. & Merloni, A. 2019, *ApJ*, 871, L6
- Kashlinsky, A., Arendt, R. G., Mather, J. & Moseley, S. H. 2005, *Nature*, 438, 45
- Kashlinsky, A., Arendt, R. G., Mather, J. & Moseley, S. H. 2007, *ApJ*, 654, L5
- Kashlinsky, A. & Rees, M. J. 1983, *MNRAS*, 205, 995
- Lacki, B. C. & Beacom, J. F. 2010, *ApJ*, 720, L67
- Laha, R. 2019, *Phys. Rev. Lett.* 123, 251101
- Liu, B., Zhang, S. & Bromm, V. 2022, *MNRAS*, 514, 2376
- Maio, U., Koopmans, L. V. E. & Ciardi, B. 2011, *MNRAS*, 412, L40
- Meszaros, P. 1975, *A&A*, 38, 5
- O'Leary, R.M. & McQuinn, M. 2012, *ApJ*, 760, 4
- Oguri, M., Diego, J.M., Kaiser, N., Kelly, P.L. & Broadhurst, T. 2018, *Phys Rev. D* 97, 023518
- Peebles, J. 1980, "The Large Scale Structure of the Universe", Princeton U.P.
- Poulin, V., Serpico, P. D., Calore, F., Clesse, S. & Kohri, K. 2017, *Phys. Rev. D*, 96, 083524
- Press, W.H. & Schechter, P. 1974, *ApJ*, 187, 425
- Richardson, M. L. A., Scannapieco, E. & Thacker, R. J. 2013, *ApJ*, 771, 81
- Seljak, U. & Zaldarriaga, M. 1996, *ApJ*, 437, 444
- Stacy, A., Bromm, V. & Loeb, A. (2011) *ApJ*, 730, L1
- Tselikhovich, D., Barkana, R. & Hirata, C. M. 2011, *MNRAS*, 418, 906
- Tselikhovich, D. & Hirata, C. 2010, *Phys Rev D*, 82, 3520

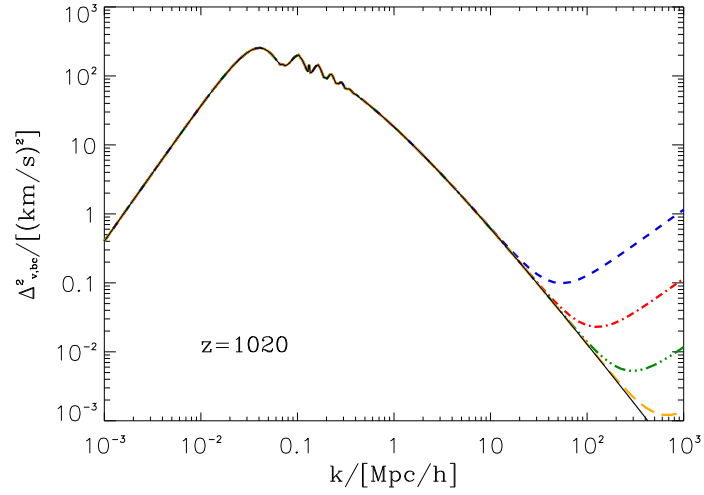


FIG. 1.— Variance of the streaming velocity field between baryons and DM. The dashed (blue), dot-dashed (red), triple dot-dashed (green) and long dashes (gold) lines also include the contribution from PBHs with fractions $f_{PBH} = (1, 0.1, 0.01, 10^{-3})$, respectively. The solid black line corresponds to the concordance Λ CDM model, i.e., $f_{PBH} = 0$.

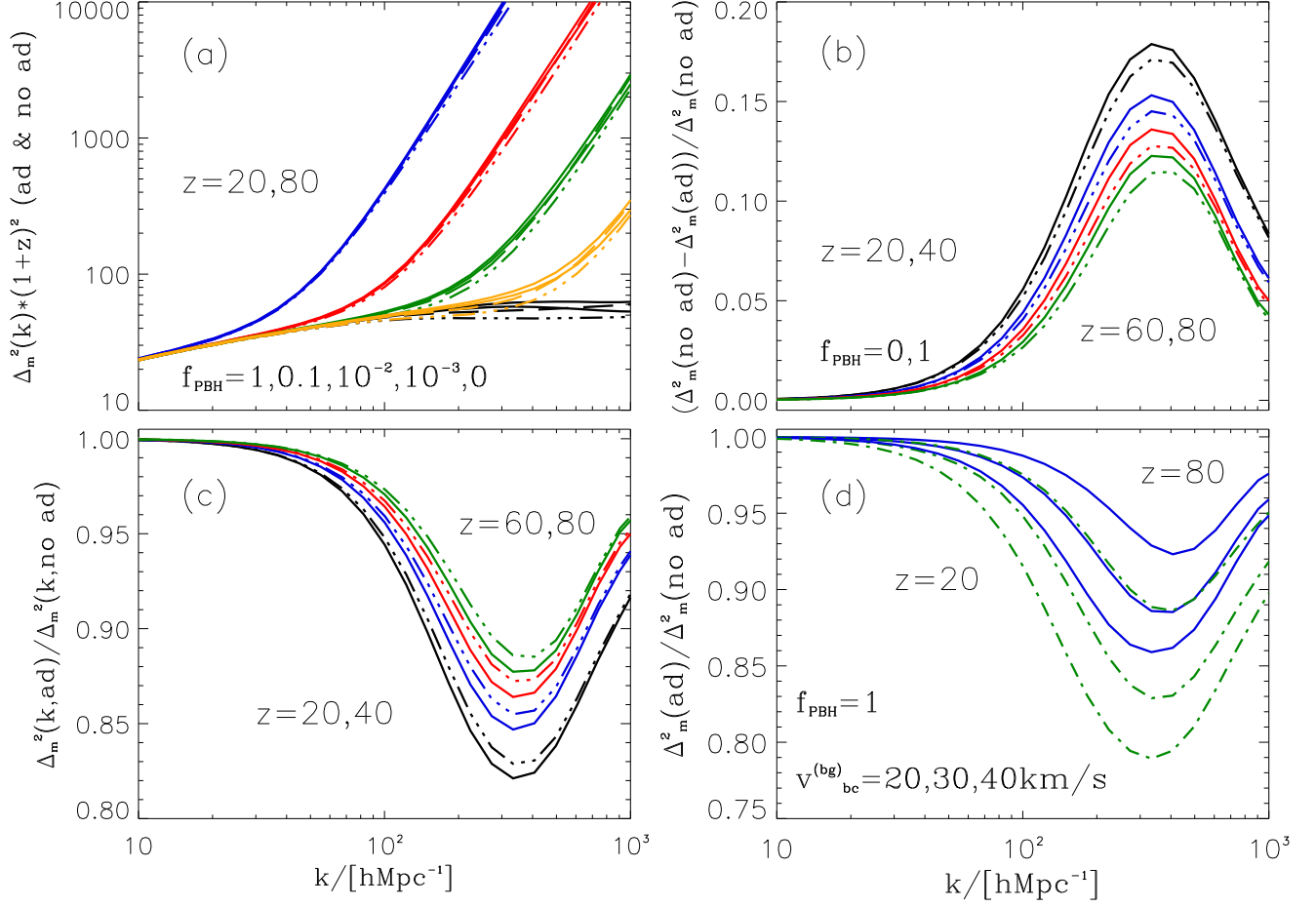


FIG. 2.— (a) Variance of the matter distribution times its redshift dependence. From left to right, blue, green, red, gold and black lines correspond to $f_{PBH} = 1, 0.1, 10^{-2}, 10^{-3}, 0$. Solid lines correspond to no-advection and broken lines to advection. Dashed lines and their nearby solid lines correspond to $z = 80$ while the triple dot-dashed lines and nearby solid lines correspond to $z = 20$. In (b) we plot the relative difference of the variance. Solid and triple dot-dashed lines correspond to $f_{PBH} = 0$ and $f_{PBH} = 1$, respectively. From top to bottom lines correspond to $z = 20$ (black), $z = 40$ (blue), $z = 60$ (red) and $z = 80$ (green). In (c) we plot the ratio of the variance with advection to variance without advection. Lines follow the same convention than in (b). In (d) we show the effect of varying the background advection velocity. The top three solid blue lines correspond to $z = 80$ and the bottom green dot-dashed ones to $z = 20$. At each redshift, the top, middle and bottom lines correspond to $v_{bc}^{(bg)} = 20, 30, 40$ km/s, respectively.

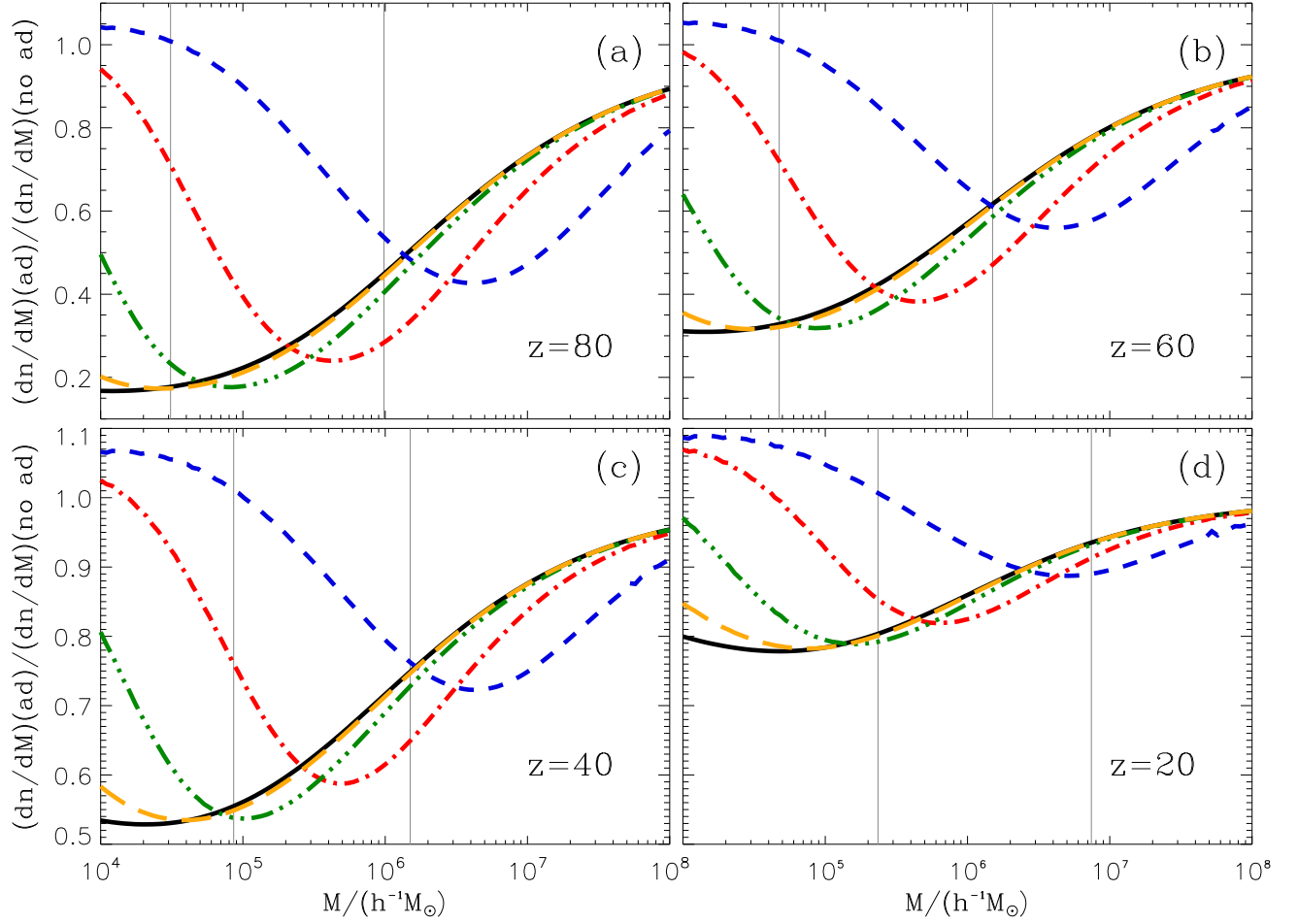


FIG. 3.— Ratio of the number density of collapsed objects per unit of total mass for models with advection to models without advection. (a) corresponds to redshift $z = 80$, (b) to $z = 60$ and (c) to $z = 40$ and (d) to $z = 20$. Dashed (blue), dot-dashed (red), triple dot-dashed (green), long dashed (gold) and solid (black) lines correspond to $f_{PBH} = 1, 0.1, 10^{-2}, 10^{-3}, 0$, respectively. The vertical gray lines correspond to the masses of halos that have reached a virial temperature $T_{vir} = 10^3$ K (left) and $T_{vir} = 10^4$ K (right).